

Dependence of the amplitude of gravitational waves from preheating on the inflationary energy scale

Rong-Gen Cai^{1,2,3,*}, Zong-Kuan Guo^{1,2,3,†}, Pei-Ze Ding^{4,‡}, Cheng-Jie Fu^{3,2,§} and Jing Liu^{1,2,¶}

¹*School of Fundamental Physics and Mathematical Sciences, Hangzhou Institute for Advanced Study, University of Chinese Academy of Sciences, Hangzhou 310024, China*

²*School of Physical Sciences, University of Chinese Academy of Sciences, No.19A Yuquan Road, Beijing 100049, China*

³*CAS Key Laboratory of Theoretical Physics, Institute of Theoretical Physics, Chinese Academy of Sciences, P.O. Box 2735, Beijing 100190, China and*

⁴*School of Gifted Young, University of Science and Technology of China, Hefei, Anhui 230026, China*

Stochastic gravitational wave backgrounds (SGWBs) receive increasing attention and provide a new possibility to directly probe the early Universe. In the preheating process at the end of inflation, parametric resonance can generate large energy density perturbations and efficiently produce gravitational waves (GWs) which carry unique information about inflation. Since the peak frequency of such GWs is approximately proportional to the inflationary energy scale, Λ_{inf} , GWs from preheating are expected to be observed by interferometer GW detectors in low-scale inflationary models. We investigate the dependence of the amplitude of such GWs on Λ_{inf} , and find that the present energy spectrum of these GWs does not depend on Λ_{inf} only in the case of Λ_{inf} is above a critical value Λ_c , a parameter depending on the resonance strength. We numerically obtain Λ_c in terms of the model parameters in linear approximation and then conduct lattice simulations to verify this result. For $\Lambda_{\text{inf}} \lesssim \Lambda_c$, the amplitude of GWs quickly decreases with Λ_{inf} and becomes challenging to observe. In turn, observing such GWs in interferometer detectors also helps to determine Λ_{inf} and the resonance strength during the preheating.

I. INTRODUCTION

Inflation is a successful model of the very early Universe which naturally solves the Horizon problem, the flatness problem, and the magnetic monopole problem simultaneously [1, 2]. Primordial curvature perturbations from quantum fluctuations during inflation also successfully explain the CMB temperature fluctuations and seed the initial value of the large scale structure [3]. The existence of primordial GWs generated from quantum fluctuations of tensor modes is an important prediction of inflation, and is expected to be detected from B-mode polarization of CMB anisotropies [4]. Since the amplitude of primordial tensor perturbations depends on Λ_{inf} (the energy scale of inflation), the upper limits of tensor perturbations help to distinguish the inflationary models [5, 6]. The current constraint from CMB data on the tensor-to-scalar ratio is $r < 0.09$ at 95% level, excluding the models with quartic and cubic potentials [7].

Apart from primordial GWs, another prediction of GWs comes from the preheating process at the end of inflation [8]. To set the initial conditions of the hot Big-Bang Universe, the vacuum energy transfers into radiation and reheats the universe after inflation, which is referred to as reheating [9, 10]. Many inflationary models predict the existence of preheating process at the

beginning of reheating, where the perturbations of the inflaton are amplified exponentially by parametric resonance, generating large energy density perturbations inside the Hubble horizon [11, 12]. During the preheating, the equation of state of the Universe, ω , could deviate from $1/3$ (in radiation-dominated Universe) or 0 (in matter-dominated Universe), depending on the form of the effective potential. Therefore, the dynamics during the preheating affect the model prediction of the e -folding numbers of inflation, the amplitude of the power spectrum of scalar perturbations and the scalar spectral index [13]. In general, preheating is expected to happen at an energy scale much higher than that colliders could reach [2, 14, 15]. GWs generated during the preheating then provide us a new opportunity to explore the end of inflation and the history of the early Universe.

The detailed dynamics of preheating is investigated by analytical and numerical methods in various models [16–24]. The case the inflaton ϕ is coupled to a scalar field χ by the term $\frac{1}{2}g^2\phi^2\chi^2$ is studied thoroughly in Ref. [11]. Ref. [25] considers GWs from tachyonic preheating after hybrid inflation. Refs. [26–28] consider the case the inflaton is coupled to gauge fields through the axion-like coupling. Refs. [29, 30] consider the amplification of perturbations and the formation oscillons in cuspy models. The parametric resonance induced by non-minimal coupling is investigated in Refs. [31–33]. However, since the comoving Hubble horizon is very small at the end of inflation, the peak frequency of such GWs is in general much higher than the sensitive frequency of the current laser interferometers [34]. For example, if Λ_{inf} is close to the grand unified theory scale, 10^{16}GeV , the peak frequency is above 10^8Hz . However, in hybrid inflation [35] and curvaton models [36], the inflationary potential is free from

*Electronic address: cairg@itp.ac.cn

†Electronic address: guozk@itp.ac.cn

‡Electronic address: peize18@mail.ustc.edu.cn

§Electronic address: fucj@itp.ac.cn

¶Corresponding author: liujing@ucas.ac.cn

the CMB constraints so that Λ_{inf} could be much smaller. In particular, taking into account the trans-Planckian-conjecture [37], Λ_{inf} should be smaller than 10^9 GeV , and then the peak frequency lies in the sensitivity bands of interferometer detectors such as aLIGO [38], DECIGO [39], LISA [40], Taiji [41] and so on.

In Ref. [34], the authors simulate GWs from preheating and find the peak value of the GW energy spectrum does not depend on Λ_{inf} . In this work, we revisit this issue in detail and find that this conjecture is valid only in the case that the parametric resonance is strong enough. We consider a broad class of models where the effective potentials have a quadratic minimum so that the resonance strength decreases with time. Since the initial value of perturbations decreases as Λ_{inf}^2 , perturbations of inflaton might remain much smaller than the background value throughout preheating in low-scale inflationary models. In this case, the energy density of perturbations is too small to generate considerable GWs. We study how the amplitude of GWs from the preheating depends on Λ_{inf} using both analytical and numerical methods in this work.

The paper is organized as follows. In Sec. II, we introduce the inflationary model investigated in this work. In Sec. III, we analyze the dynamics of preheating in the linear approximation. In Sec. IV, we show the results of the present energy spectrum of GWs from lattice simulation and compare them with the results in linear analysis. In Sec. V, we summarize the results. We set $c = 8\pi G = 1$ throughout the paper.

II. MODELS

In this section, we briefly introduce the model investigated in this work.

Consider the model realized by the following action,

$$S = \int d^4x \sqrt{-g} \left(-\frac{1}{2}R + \frac{1}{2}\partial_\mu\phi\partial^\mu\phi + V(\phi) \right), \quad (1)$$

where R is the Ricci scalar, ϕ could be, for example, the inflaton in curvaton models or the waterfall field in hybrid inflationary models. Since ϕ is not responsible to generate primordial perturbations and explain the CMB temperature fluctuations observed by Planck, $V(\phi)$ is free from CMB constraints. We investigate the SGWB from the preheating in the α -attractor E-model, where the effective potential reads

$$V(\phi) = V_0 \left[1 - \exp\left(-\frac{\phi}{M}\right) \right]^2, \quad (2)$$

where M and V_0 are free parameters. Assuming the energy density during inflation is approximately a constant, then $\Lambda_{\text{inf}} = V_0^{\frac{1}{4}}$. In the limit $\phi \rightarrow 0$, potential (2) tends to be quadratic, $V(\phi) \simeq \frac{1}{2}m^2\phi^2$, where the effective mass $m = \sqrt{V_0}/M$.

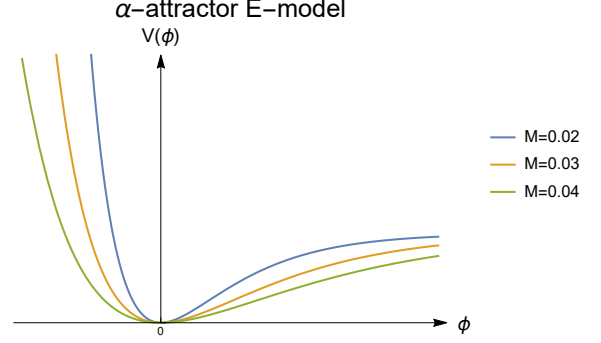


FIG. 1: The effective potential of α -attractor E-models.

In a Friedmann-Lemaître-Robertson-Walker Universe, the Friedman equation and the equation of motion (EOM) of ϕ are

$$\begin{aligned} H^2 &= \frac{1}{3} \left\langle \frac{1}{2}\dot{\phi}^2 + \frac{1}{2a^2}(\nabla\phi)^2 + V(\phi) \right\rangle, \\ \ddot{\phi} - \frac{1}{a^2}\nabla^2\phi + 3H\dot{\phi} + \frac{dV}{d\phi} &= 0, \end{aligned} \quad (3)$$

where H is the Hubble parameter, $\langle \dots \rangle$ denotes a spatial average over the volume, overdots denote derivatives with respect to the cosmic time t , and ∇ is the spatial gradient. The quantity inside the angle bracket presents the energy density of ϕ . The EOM of tensor perturbations, h_{ij} , is derived from the linearized Einstein equation

$$\ddot{h}_{ij} + 3H\dot{h}_{ij} - \frac{1}{a^2}\nabla^2 h_{ij} = \frac{2}{M_{\text{pl}}^2 a^2} T_{ij}^{\text{TT}}, \quad (4)$$

where T_{ij}^{TT} is the transverse-traceless (TT) component of the energy-momentum tensor T_{ij} , which takes the form

$$T_{ij} = \partial_i\phi\partial_j\phi - \frac{1}{3}\delta_{ij}\partial_k\phi\partial^k\phi. \quad (5)$$

In general, the resonance wavelength is more than two orders of magnitude smaller than the Hubble horizon scale, so scalar metric perturbations are negligible both in the EOMs of ϕ and h_{ij} .

The energy density of GWs is given by

$$\rho_{\text{GW}} = \frac{1}{4} \langle \dot{h}_{ij} \dot{h}^{ij} \rangle, \quad (6)$$

and the dimensionless energy spectrum of GWs is defined by

$$\Omega_{\text{GW}} \equiv \frac{1}{\rho_c} \frac{d\rho_{\text{GW}}}{d \ln k}, \quad (7)$$

where ρ_c is the critical density of the Universe.

III. LINEAR APPROXIMATION

In this section, we investigate the dynamics of perturbations in the linear approximation and then give the results of Λ_c in terms of M from the linear analysis.

After inflation, ϕ begins to oscillate around the minimum of its potential. At the beginning of preheating, ϕ is almost homogeneous with some small perturbations on it caused by quantum fluctuations. Thus, we split $\phi(\mathbf{x})$ as small fluctuations around a homogeneous field, $\phi(t, \mathbf{x}) = \bar{\phi}(t) + \delta\phi(t, \mathbf{x})$. The EOMs of $\bar{\phi}$ and $\delta\phi$ are

$$\ddot{\bar{\phi}} + 3H\dot{\bar{\phi}} + \frac{dV}{d\bar{\phi}} = 0, \quad (8)$$

$$\delta\ddot{\phi}_k + \frac{k^2}{a^2}\delta\phi_k + 3H\delta\dot{\phi}_k + \frac{d^2V}{d\bar{\phi}^2}\delta\phi_k = 0, \quad (9)$$

where $\delta\phi_k$ is the fourier form of $\delta\phi(\mathbf{x})$.

Since the energy density of $\delta\phi$ is negligible at the beginning of preheating, the Hubble parameter is calculated from the energy density of $\bar{\phi}$. Thus, the EOM of $\bar{\phi}$ can be solved independently assuming field fluctuations have little effect on it. In the linear analysis, each Fourier mode of fluctuations evolves independently so that Eq. (9) can be numerically solved as an ordinary differential equation.

As an illustration, in linear analysis we choose $\bar{\phi}_i = 2M$ and $\dot{\bar{\phi}}_i = 0$ as the initial conditions for the homogeneous field. The subscript i denotes the initial value of the variables at the beginning of preheating throughout this paper. The initial value of perturbations is obtained as the Bunch-Davies type

$$\delta\phi_{k,i} = \frac{1}{\sqrt{2k}}e^{ik\eta}, \quad (10)$$

where η is the conformal time. The expression (10) is equivalent to the estimation of quantum kicks, $\delta\phi_i \sim H_{\text{inf}}/(2\pi)$. Since $H_{\text{inf}}^2 = \Lambda_{\text{inf}}^4/3$, $\delta\phi_i$ is proportional to Λ_{inf}^2 , and thus the initial value of perturbations is smaller in low-scale inflationary models.

If we firstly neglect the expansion of the Universe, the oscillation amplitude of $\bar{\phi}$ is a constant so that Eq. (9) is periodic in Minkowski space. Then, according to the Floquet theory, the periodic equation (9) has a general solution

$$\delta\phi_k = \mathcal{P}_{k+}(t)\exp(\mu_k t) + \mathcal{P}_{k-}(t)\exp(-\mu_k t), \quad (11)$$

where μ_k is the Floquet exponent and $\mathcal{P}_{k\pm}$ are periodic functions determined by initial conditions.

In that case that the real part of μ_k is nonzero, i.e., $\text{Re}(\mu_k) \neq 0$, perturbations are unstable and $\delta\phi_k$ grows exponentially.

We use the rescaled wavenumber $\kappa \equiv k/\sqrt{V_0}$ and rescaled time $\tau \equiv t\sqrt{V_0}$ so that the resonant modes satisfy $\kappa \sim \mathcal{O}(1) - \mathcal{O}(10^3)$ and the preheating process sus-

tains for about $\tau \sim \mathcal{O}(10^2)$. The left panel of Fig. 2 shows the dependence of $|\text{Re}(\mu_k)|$ on κ and ϕ_i , one can find that $|\text{Re}(\mu_k)|$ is close to zero for $\phi_i \ll M$. This is because the potential is proportional to ϕ^2 at its bottom, then Eq. (9) implies $\delta\phi$ could be treated as a free massive particle and the amplification of perturbations does not occur. As a result, the resonance strength decreases with the oscillation amplitude of $\bar{\phi}$ in the expanding Universe. For smaller M , the resonance is stronger because the effective mass m becomes larger and $\bar{\phi}$ oscillates more times in unit time. One can find the resonance band is wider and $|\text{Re}(\mu_k)|$ is larger for smaller M in the left panel of Fig. 2.

When the oscillation amplitude of $\bar{\phi}$ becomes much smaller than M , Eqs. (8) and (9) suggest that both $\bar{\phi}$ and $\delta\phi$ behave as massive particles with effective mass m , and their amplitude decreases as $a^{-3/2}$. Then, we use $\bar{\varphi} \equiv a^{3/2}\bar{\phi}$ and $\delta\varphi \equiv a^{3/2}\delta\phi$ instead to include the effect of the expansion of the Universe.

In Fig. 3 we show the evolution of $\langle\delta\varphi_{\mathbf{k}}^2\rangle$, which implies $\langle\delta\varphi_{\mathbf{k}}^2\rangle$ increases for about 10^{18} and finally tends to be a constant. The right panel of Fig. 2 shows $\langle\delta\varphi_{\mathbf{k}}^2\rangle/\langle\delta\varphi_{\mathbf{k},i}^2\rangle$ in terms of M and κ at the end of resonance.

To quantify the amplitude of perturbations, we apply the variance of $\delta\varphi$, $\langle\delta\varphi^2\rangle$, which is defined as

$$\langle\delta\varphi^2\rangle \equiv \frac{1}{\mathcal{V}} \int d^3x |\delta\varphi(\mathbf{x})|^2 = \int \frac{d^3k}{(2\pi)^3} |\delta\varphi_{\mathbf{k}}|^2, \quad (12)$$

where \mathcal{V} is the volume of the integration region. Since the resonance is only efficient in a limited time, the amplification of $\langle\delta\varphi^2\rangle$ during preheating has an upper bound. In other words, if we put aside the nonlinear effects and solve Eq. (9) under the linear approximation, there is a maximum value $\langle\delta\varphi^2\rangle$ which could finally reach at the end of resonance, denoted as $\langle\delta\varphi^2\rangle_m$. But the linear approximation is violated when $\delta\phi$ is comparable to $\bar{\phi}$. At that time, the oscillation amplitude of $\bar{\phi}$ quickly decreases, Eq. (9) is violated and we need to conduct lattice simulations to capture the nonlinear dynamics of preheating. Depending on the value of $\delta\phi_i$, the system will become nonlinear at different times or remains in the linear stage if $\delta\phi_i$ is too small. We assume the system becomes nonlinear when $\langle\delta\phi^2\rangle$ exceeds $\bar{\phi}^2$. The case is then referred to as sufficient/insufficient preheating when the evolution of the system becomes nonlinear/remains linear at the end of resonance. The left panel of Fig. 4 shows that $\langle\delta\varphi^2\rangle_m/\Lambda_{\text{inf}}^4$ increases inversely with M , which agrees with the results shown in Fig. 2 that $|\text{Re}(\mu_k)|$ is larger for smaller M . Then, the threshold Λ_c can be obtained by considering the case $\delta\phi$ just reaches the nonlinear condition $\langle\delta\phi^2\rangle_m = \bar{\phi}_i$ at the end of resonance, as shown in the right panel of Fig. 4.

As for the amplitude of GWs, it is natural to expect that in the sufficient preheating case the energy density perturbations are amplified to the maximum value by nonlinear evolution, so that the amplitude of GWs remains the same. In the insufficient preheating case, most

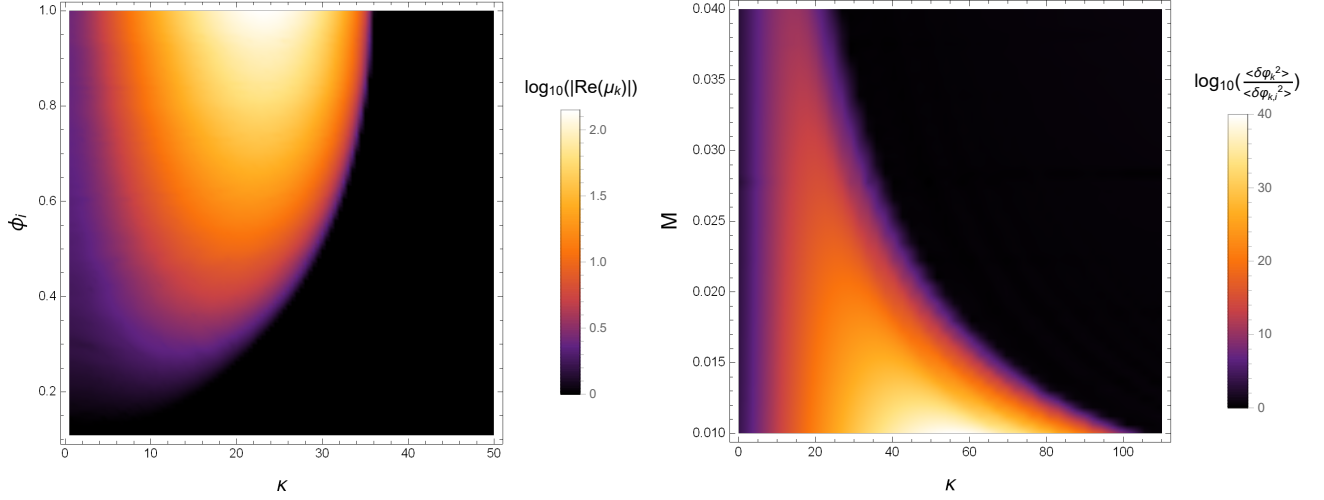


FIG. 2: Left: The resonance strength $|\text{Re}(\mu_k)|$ in terms of ϕ_i and κ in case of $M = 0.02$. Right: $\langle \delta \varphi_k^2 \rangle / \langle \delta \varphi_{k,i}^2 \rangle$ in terms of M and κ at the end of resonance.

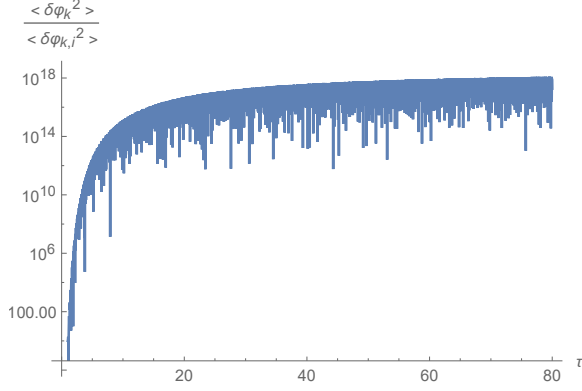


FIG. 3: The amplification of $\langle \delta \varphi_k^2 \rangle$, where we choose $\kappa = 20$ and $M = 0.02$.

of the energy remains storing in the homogeneous part of the scalar field at the end of resonance. Since GWs are generated by the TT part of the energy density, without sufficient amplification of perturbations, the GW production is expected to be suppressed.

Eq. (4) implies that h_{ij} is proportional to the source term, $\partial_i \phi \partial_j \phi$, which is quadratically dependent of $\delta \phi$. So we simply assume $h_{ij} \propto \langle \delta \phi^2 \rangle_m$ and $\Omega_{\text{GW}} \propto \langle \delta \phi^2 \rangle_m^2$ in the insufficient preheating case. Since the amplification rate of $\langle \delta \phi^2 \rangle$ is a constant in this case, i.e., $\langle \delta \phi^2 \rangle_m \propto \langle \delta \phi_i^2 \rangle$, Ω_{GW} is further proportional to $\langle \delta \phi_i^2 \rangle^2$. Using the relation $\delta \phi_i \sim H_{\text{inf}}/(2\pi)$, we can obtain the dependence of Ω_{GW} on Λ_{inf} as

$$\Omega_{\text{GW}} = \begin{cases} \Omega_{\text{max}}, & \text{for } \Lambda_{\text{inf}} \geq \Lambda_c, \\ \Omega_{\text{ins}}(\Lambda_{\text{inf}}/\Lambda_c)^8, & \Lambda_{\text{inf}} \ll \Lambda_c, \end{cases} \quad (13)$$

where Ω_{max} and Ω_{ins} are the maximum values that Ω_{GW} could reach in the sufficient preheating case and the insufficient preheating case, respectively. Intuitively speak-

ing, GWs should be stronger in sufficient preheating case, i.e., $\Omega_{\text{max}} \geq \Omega_{\text{ins}}$. For $\Lambda_{\text{inf}} > \Lambda_c$, Ω_{GW} is independent of Λ_{inf} . For $\Lambda_{\text{inf}} < \Lambda_c$, Ω_{GW} quickly decreases and becomes more difficult to be observed. This analytical result will be compared with the lattice simulation result in the next section. Note that in Eq. (13) there is a huge difference between Ω_{max} and Ω_{ins} , which implies Ω_{GW} has a sudden change near $\Lambda_{\text{inf}} = \Lambda_c$, which is also stressed in the next section.

IV. LATTICE SIMULATIONS

In this section, we present the numerical methods used in lattice simulation, and the numerical results of the present energy spectrum of GWs, $\Omega_{\text{GW},0}$, for different M and Λ_{inf} . Then, we show the dependence of $\Omega_{\text{GW},0}$ on Λ_{inf} from lattice simulation, and compare with the results in the linear analysis.

When perturbations become comparable to the homogeneous part, nonlinear effects cannot be neglected and the evolution of ϕ has to be solved in lattice simulations. To improve computational accuracy of the simulations, we apply the redefined variables as in LATTICEASY [42] and DEFROST [43], which are given by

$$\phi_{\text{pr}} = a^{3/2} \phi / \phi_i, \quad dt_{\text{pr}} = dt \sqrt{V_0} / M, \quad k_{\text{pr}} = k M / \sqrt{V_0}. \quad (14)$$

We apply the finite-difference method to solve the EOMs of ϕ and h_{ij} in configuration space, both the spacial derivatives and the time derivatives are realized using the fourth-order method with double precision. Also, we use a performance-portable parallel programming model, OPENACC, to accelerate the code with GPUs.

To reduce the computational cost of the simulation,

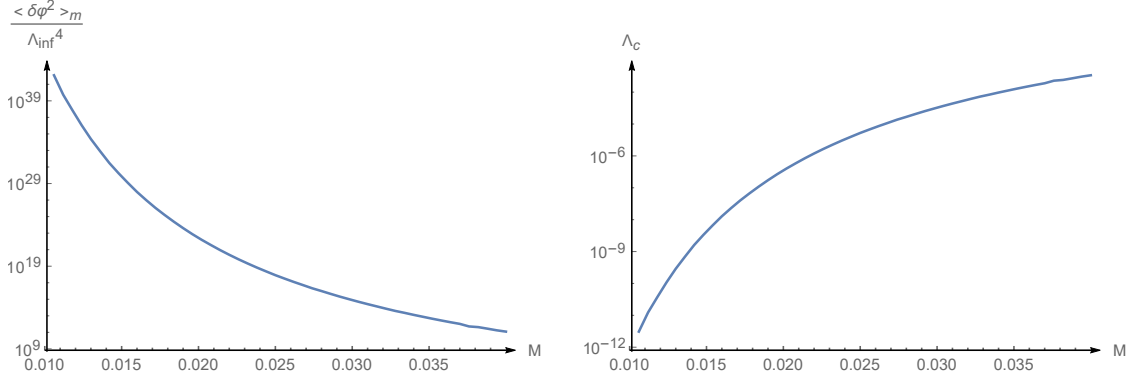


FIG. 4: Left: $\langle \delta\phi^2 \rangle_m / \Lambda_{\text{inf}}^4$ in terms of M . Right: Λ_c in terms of M from linear analysis.

we have defined a new quantity u_{ij} , and the EOM of u_{ij} reads

$$\ddot{u}_{ij} + 3H\dot{u}_{ij} - \frac{1}{a^2}\nabla^2 u_{ij} = \frac{2}{a^2}T_{ij}. \quad (15)$$

Then, h_{ij} can be obtained by conduct the TT projection on u_{ij}

$$h_{ij}(t, \mathbf{k}) = \Lambda_{ij,lm}(\hat{\mathbf{k}})u_{lm}(t, \mathbf{k}), \quad (16)$$

where $u_{lm}(t, \mathbf{k})$ is the Fourier form of u_{ij} and the projection operator $\Lambda_{ij,lm}(\hat{\mathbf{k}})$ reads

$$\Lambda_{ij,lm}(\hat{\mathbf{k}}) \equiv P_{il}(\hat{\mathbf{k}})P_{jm}(\hat{\mathbf{k}}) - \frac{1}{2}P_{ij}(\hat{\mathbf{k}})P_{lm}(\hat{\mathbf{k}}), \quad (17)$$

with $P_{ij} \equiv \delta_{ij} - \hat{k}_i\hat{k}_j$. Thus, one needs to conduct the TT projection on u_{ij} only at the times exporting the value of Ω_{GW} , and avoids the calculation of the TT projection at each step.

Similar to the EOM of the ϕ , we thus can evolve Eq. (15) in configuration space in the simulations. In terms of u_{ij} , Ω_{GW} then can be expressed as [44]

$$\Omega_{\text{GW}} = \frac{k^3}{4L^3\rho_c} \int d\Omega \Lambda_{ij,lm}(\hat{\mathbf{k}})\dot{u}_{ij}(t, \mathbf{k})\dot{u}_{lm}^*(t, \mathbf{k}). \quad (18)$$

The expansion rate of the Universe is calculated self-consistently from spatially averaged energy density. We perform three-dimensional lattice simulations with 256^3 points in a box with periodic boundary conditions. The size of the box L and the number of grid points per edge N are in principle chosen according to the physical features of the model. In our simulations, the box size is chosen to be close to the resonance wavelength, which is smaller than the Hubble horizon size, so that the interesting wavelengths such as the physical peaks in Ω_{GW} are located comfortably in between the largest wavelength $\sqrt{3}L$ (diagonal line) and the smallest wavelength L/N .

The initial values of $\bar{\phi}$ and $\delta\phi$ are the same as in Sec. III. The evolution of Ω_{GW} from lattice simulations is shown in Fig. 5, where Ω_{GW} is exported every $\Delta\tau = 100$

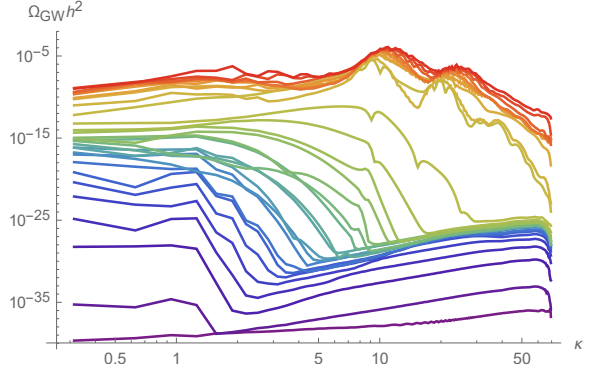


FIG. 5: The evolution of Ω_{GW} in case of $M = 0.02$ and $\Lambda_{\text{inf}} = 3.8 \times 10^{-7}$. The data is exported for every $\Delta\tau = 100$ and the program ends at $\tau = 3000$ when Ω_{GW} stops increasing.

and the simulation ends at $\tau = 3000$ when Ω_{GW} stops increasing. The evolution of Ω_{GW} has experienced roughly three stages, as also mentioned in Ref. [18]. Firstly, the increase of Ω_{GW} appears only in the low- k region, corresponding to the resonant amplification of perturbations in the linear stage. Secondly, the nonlinear effects starts to dominate the evolution, and in the high- k region Ω_{GW} quickly increases. Thirdly, the nonlinear evolution is fully established, the compact objects, oscillons form [45–47] and Ω_{GW} gradually stops increasing. The two peaks of Ω_{GW} appear in the high- k region as a consequence of oscillons.

To estimate $\Omega_{\text{GW},0}$ and the corresponding frequency f , we assume the thermal equilibrium is established shortly after the end of the simulation. Since the energy density of radiation evolves as $\rho_r \propto g^{-1/3}a^{-4}$, $\Omega_{\text{GW},0}$ and the frequency f read

$$\Omega_{\text{GW},0} = \Omega_{r,0} \left(\frac{g_0}{g_*} \right)^{1/3} \Omega_{\text{GW}}, \quad (19)$$

$$f \simeq \frac{k}{a_e \Lambda_{\text{inf}}} \left(\frac{g_0}{g_*} \right)^{1/12} 4 \times 10^{10} \text{ Hz}, \quad (20)$$

where $\Omega_{r,0}$ is the density fraction of radiation at present, a_e is the scale factor at the end of the simulation, and g_0 and g_e are the effective numbers of ultrarelativistic degree of freedoms at present and at the end of the simulation, respectively.

In Fig. 6 we show the dependence of $\Omega_{\text{GW},0}$ on Λ_{inf} in the case of $M = 0.02$, $M = 0.03$, $M = 0.04$, respectively. The values of Λ_c are obtained from the linear analysis in Sec. III. For $M = 0.02$, $\Lambda_c = 3.8 \times 10^{-7}$, for $M = 0.03$, $\Lambda_c = 3.3 \times 10^{-5}$, for $M = 0.04$, $\Lambda_c = 3.0 \times 10^{-4}$, respectively. The green thick line in each panel of Fig. 6 shows the predicted $\Omega_{\text{GW},0}$ for $\Lambda_{\text{inf}} = \Lambda_c$. Fig. 6 shows that the peak values of $\Omega_{\text{GW},0}$ are almost constant for $\Lambda_{\text{inf}} > \Lambda_c$, corresponding to the sufficient preheating case, and quickly decreases for $\Lambda_{\text{inf}} < \Lambda_c$, corresponding to the insufficient preheating case. The peak frequency is roughly proportional to Λ_{inf} , and $\Omega_{\text{GW},0}$ is proportional to f^8 for $\Lambda_{\text{inf}} < \Lambda_c$. Thus, the lattice results verify the result (13) in the linear analysis.

As shown in Fig. 7, the accurate value of Λ_c is between 2.14×10^{-7} to 1.20×10^{-7} for $M = 0.02$, where $\Omega_{\text{GW},0}$ suddenly decreases when Λ_{inf} becomes slightly smaller than Λ_c . The profile of $\Omega_{\text{GW},0}$ with $\Lambda_{\text{inf}} = 2.14 \times 10^{-7}$ and $\Lambda_{\text{inf}} = 1.20 \times 10^{-7}$ are different, where the former peaks at high- k region while the latter exhibits a plateau in the low- k region. Let us recall the evolution of Ω_{GW} in Fig. 5. The profile of Ω_{GW} for $\Lambda_{\text{inf}} = 2.14 \times 10^{-7}$ and $\Lambda_{\text{inf}} = 1.20 \times 10^{-7}$ respectively correspond to Ω_{GW} in the linear stage and fully nonlinear stage. This is shown more clearly by the two-dimensional slices of energy density perturbations in the lower panel of Fig. 7. The system remains in the linear stage for $\Lambda_{\text{inf}} = 1.20 \times 10^{-7}$, while the nonlinear evolution is fully established for $\Lambda_{\text{inf}} = 2.14 \times 10^{-7}$. By comparing the evolution of energy density perturbations and Ω_{GW} , we conclude that GWs are many orders of magnitude enhanced by nonlinear evolution. Fig. 7 implies that once energy perturbations reach a certain threshold, the system will ultimately evolve into the fully nonlinear stage, even if the resonance becomes very weak. From Fig. 7 one also finds that the length scale of perturbations becomes smaller in nonlinear evolution, corresponding to the increase of the GW peak frequency in the nonlinear stage.

In model (2), the effective mass at the bottom of the potential is proportional to M^{-1} . As a result, $\bar{\phi}$ oscillates more rapidly as M decreases and the energy stored in $\bar{\phi}$ tends to transfer into perturbations with smaller wavelengths. $\Omega_{\text{GW},0}$ also decreases as M^2 as shown in Ref. [19]. Thus, on the one hand, M needs to be small enough to trigger nonlinear evolution in low-scale inflationary models. On the other hand, decreasing M makes Ω_{max} smaller and difficult to detect. For example, the most sensitive frequency of aLIGO is about 30Hz. We need $\Lambda_c < 10^{-11}$ to guarantee sufficient preheating takes place in the case the peak frequency is below 30Hz. Using the result in Fig. 4, this condition gives an upper bound to the parameter $M \lesssim 0.011$, and thus Ω_{max} is also constrained. According to the simulation results,

$\Omega_{\text{max}} \simeq 3 \times 10^{-9}$ for $M = 0.02$, and $\Omega_{\text{max}} \simeq 1.5 \times 10^{-8}$ for $M = 0.04$, which is in constant with the analytical result $\Omega_{\text{max}} \propto M^2$ in Ref. [19]. Using this relation, Ω_{max} is estimated as 7×10^{-10} for $M \simeq 0.01$, it is also the maximum of Ω_{max} aLIGO could detect in model (2). In turn, detecting the peak frequency and the amplitude of GWs can help us determine Λ_{inf} and M .

V. CONCLUSION AND DISCUSSION

In this paper, we investigate the SGWB generated during preheating and the dependence of Ω_{GW} on Λ_{inf} . We find Ω_{GW} does not depend on Λ_{inf} only if Λ_{inf} is larger than a critical value Λ_c . Since the initial value of $\delta\phi$ decreases as Λ_{inf}^2 , for $\Lambda_{\text{inf}} < \Lambda_c$ the resonance is not strong enough to amplify $\delta\phi/\bar{\phi}$ to unity before the resonance ends, and the system stays in the linear stage. Inversely, for $\Lambda_{\text{inf}} > \Lambda_c$ the resonance is strong enough, nonlinear evolution is fully established and Ω_{GW} does not depend on Λ_{inf} . We obtain Λ_c in terms of M in linear analysis, and confirm it later by the lattice simulations. Numerical results also show that, for Λ_{inf} slightly smaller than Λ_c , Ω_{GW} suddenly decreases more than ten orders of magnitude, and becomes challenging to be observed. We can find that Ω_{GW} is immensely enhanced in nonlinear evolution by comparing the energy density distribution in both $\Lambda_{\text{inf}} \lesssim \Lambda_c$ and $\Lambda_{\text{inf}} \gtrsim \Lambda_c$ cases. For $\Lambda_{\text{inf}} \ll \Lambda_c$, Ω_{GW} is lower than 10^{-20} and proportional to Λ_{inf}^8 .

The peak frequency of GWs from the preheating also provides useful information about Λ_{inf} . As the trans-Planckian censorship conjecture suggests, Λ_{inf} should be lower than 10^{10}GeV . In this case, the peak frequency is lower than 10^4Hz , and GWs from the preheating are expected to be observed by interferometer observers such as LIGO, LISA, Taiji, DECIGO. Our work suggests that observing such GWs also gives constraints to the resonance strength and the model parameters.

In preheating models where the potential is not quartic at the bottom, it is a common feature that the resonance strength decreases with time, and the analysis in this work is applicable to many preheating models. As shown in Ref. [48], with the expansion of the Universe the k -mode could stay in the resonance band only in the case $V(\phi) \propto \phi^4$ at the bottom. In other cases, for example, $V(\phi) \propto \phi^2$ or ϕ^6 at the bottom, either the resonance bands disappears for $\phi \rightarrow 0$ or the modes are quickly redshifted out of the resonance bands. Hence, the resonance becomes weaker as the oscillation amplitude of $\bar{\phi}$ decreases, similar to the case considered in this work.

As mentioned in Sec. IV, $\Omega_{\text{GW},0}$ decreases quadratically with M , and the value of $\Omega_{\text{GW},0}$ LIGO could observe is less than about 7×10^{-10} because of the constraint $M < 0.011$. For a smaller M , it is more difficult to observe GWs from the preheating. In comparison, for the models considered in our previous work, Ω_{max} does not depend on model parameters. These models, inspired by string theory [49, 50], have a characteristic cusp in the

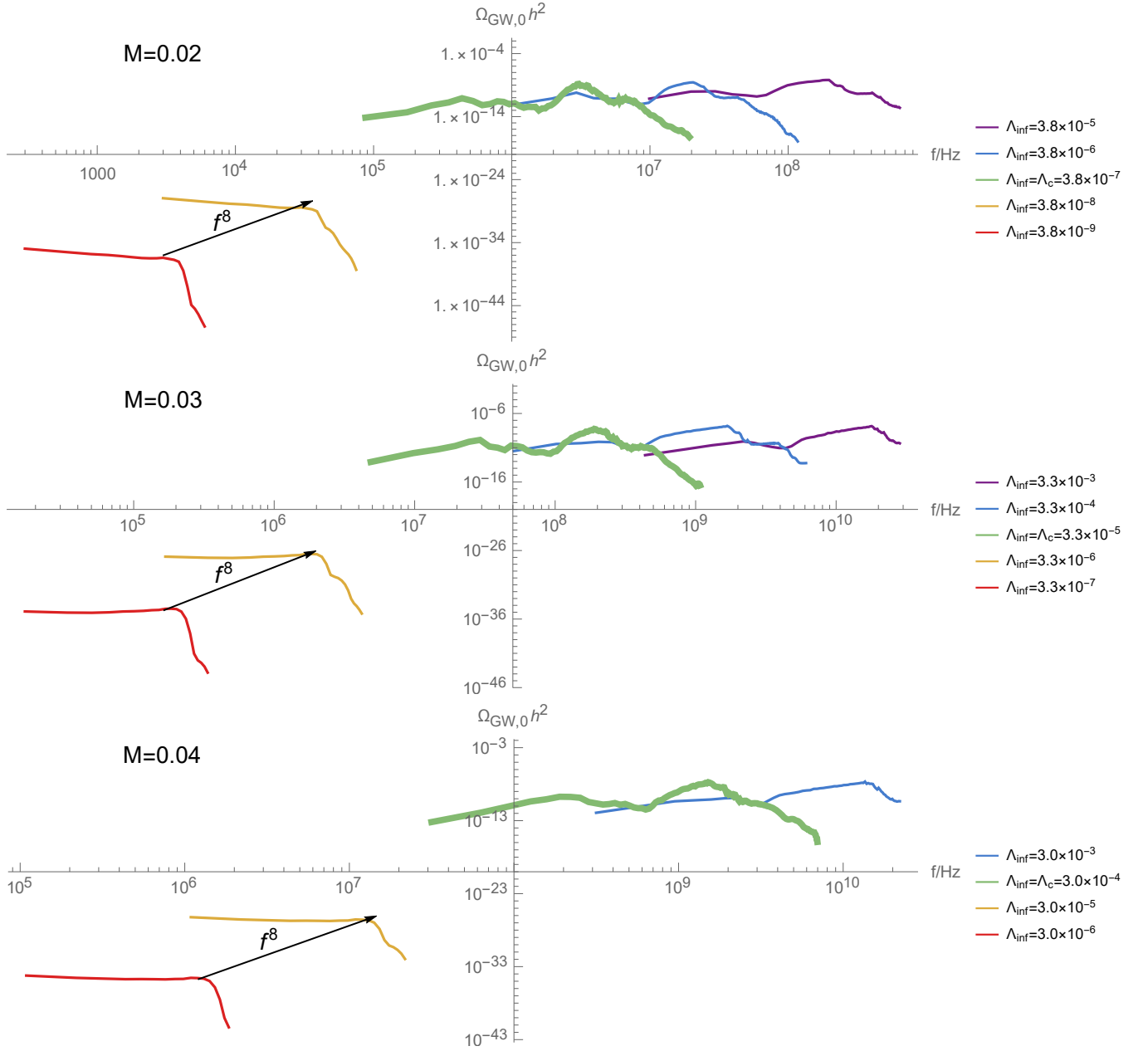


FIG. 6: The dependence of $\Omega_{\text{GW},0}$ on Λ_{inf} for $M = 0.02$, $M = 0.03$ and $M = 0.04$ case, where the thick green line in each panel denotes the result for $\Lambda_{\text{inf}} = \Lambda_c$ predicted in the Sec. III.

bottom, and GWs from the preheating in those models tends to be more strong.

Acknowledgments

This work is supported in part by the National Key Research and Development Program of China Grant No.2020YFC2201501, in part by the National Natural

Science Foundation of China Grants No. 11435006, No. 11647601, No. 11690021, No. 11690022, No. 11821505, No. 11851302, No. 12047503, No. 11991052, No. 12075297, No. 12075298, No. 11947302, No. 12047559, in part by the China Postdoctoral Science Foundation under Grant No.2020M680689, in part by the Strategic Priority Research Program of the Chinese Academy of Sciences Grant No. XDB23030100 and by Key Research Program of Frontier Sciences, CAS.

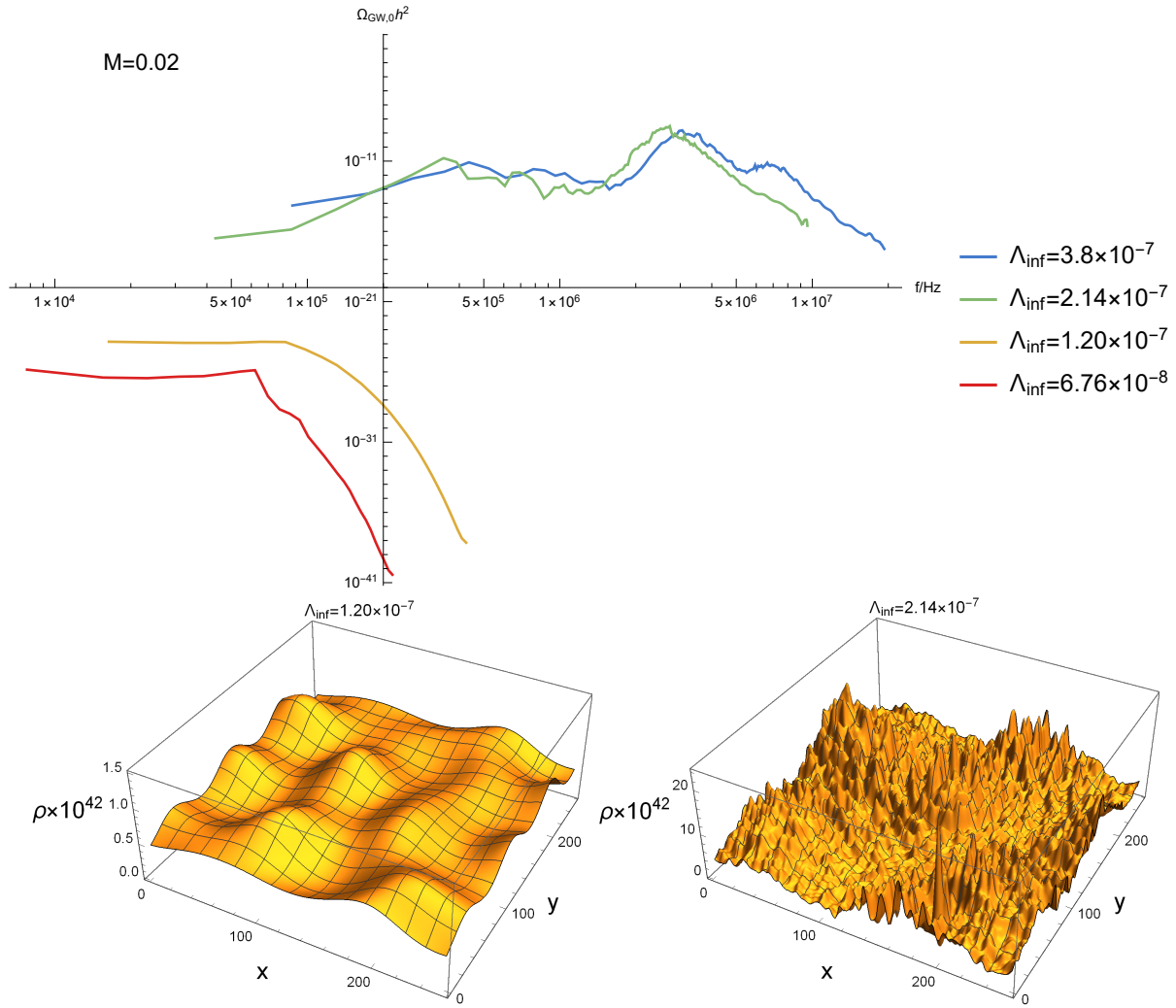


FIG. 7: Top: the dependence of $\Omega_{\text{GW},0}$ on Λ_{inf} for $M = 0.02$. $\Omega_{\text{GW},0}$ suddenly decreases for about 15 orders of magnitude when Λ_{inf} decreases from 2.14×10^{-7} to 1.20×10^{-7} . Bottom: the two-dimensional slices of energy density perturbations, where energy density perturbations are larger in $\Lambda_{\text{inf}} = 2.14 \times 10^{-7}$ case.

-
- [1] A. H. Guth, Phys. Rev. **D23**, 347 (1981), [reprint: Adv. Ser. Astrophys. Cosmol.3,139(1987)].
 - [2] A. D. Linde, Phys. Lett. **129B**, 177 (1983).
 - [3] N. Aghanim et al. (Planck), Astron. Astrophys. **641**, A6 (2020), 1807.06209.
 - [4] U. Seljak and M. Zaldarriaga, Phys. Rev. Lett. **78**, 2054 (1997), astro-ph/9609169.
 - [5] A. R. Liddle, Phys. Rev. **D49**, 739 (1994), astro-ph/9307020.
 - [6] Z.-K. Guo, D. J. Schwarz, and Y.-Z. Zhang, Phys. Rev. **D83**, 083522 (2011), 1008.5258.
 - [7] Y. Akrami et al. (Planck), Astron. Astrophys. **641**, A10 (2020), 1807.06211.
 - [8] S. Y. Khlebnikov and I. I. Tkachev, Phys. Rev. **D56**, 653 (1997), hep-ph/9701423.
 - [9] A. Albrecht, P. J. Steinhardt, M. S. Turner, and F. Wilczek, Phys. Rev. Lett. **48**, 1437 (1982).
 - [10] Y. Shtanov, J. H. Traschen, and R. H. Brandenberger, Phys. Rev. **D51**, 5438 (1995), hep-ph/9407247.
 - [11] L. Kofman, A. D. Linde, and A. A. Starobinsky, Phys. Rev. **D56**, 3258 (1997), hep-ph/9704452.
 - [12] T. Zhu, Q. Wu, and A. Wang (2018), 1811.12612.
 - [13] K. D. Lozanov and M. A. Amin, Phys. Rev. Lett. **119**, 061301 (2017), 1608.01213.
 - [14] A. A. Starobinsky, Phys. Lett. **91B**, 99 (1980), [Adv. Ser. Astrophys. Cosmol.3,130(1987)].
 - [15] V. F. Mukhanov and G. V. Chibisov, JETP Lett. **33**, 532 (1981), [Pisma Zh. Eksp. Teor. Fiz.33,549(1981)].
 - [16] P. B. Greene, L. Kofman, A. D. Linde, and A. A. Starobinsky, Phys. Rev. **D56**, 6175 (1997), hep-ph/9705347.
 - [17] G. N. Felder, J. Garcia-Bellido, P. B. Greene, L. Kofman, A. D. Linde, and I. Tkachev, Phys. Rev. Lett. **87**, 011601 (2001), hep-ph/0012142.

- [18] S.-Y. Zhou, E. J. Copeland, R. Easther, H. Finkel, Z.-G. Mou, and P. M. Saffin, *JHEP* **10**, 026 (2013), 1304.6094.
- [19] K. D. Lozanov and M. A. Amin, *Phys. Rev.* **D99**, 123504 (2019), 1902.06736.
- [20] Y. Sang and Q.-G. Huang, *Phys. Rev.* **D100**, 063516 (2019), 1905.00371.
- [21] K. Wang and Q.-G. Huang (2021), 2102.03084.
- [22] T. Hiramatsu, E. I. Sfakianakis, and M. Yamaguchi, *JHEP* **03**, 021 (2021), 2011.12201.
- [23] D. G. Figueroa, A. Florio, F. Torrenti, and W. Valkenburg (2020), 2006.15122.
- [24] S. Antusch, F. Cefala, S. Krippendorf, F. Muia, S. Orani, and F. Quevedo, *JHEP* **01**, 083 (2018), 1708.08922.
- [25] J.-F. Dufaux, G. Felder, L. Kofman, and O. Navros, *JCAP* **0903**, 001 (2009), 0812.2917.
- [26] P. Adshead, J. T. Giblin, and Z. J. Weiner, *Phys. Rev.* **D98**, 043525 (2018), 1805.04550.
- [27] J. R. C. Cuissa and D. G. Figueroa, *JCAP* **1906**, 002 (2019), 1812.03132.
- [28] P. Adshead, J. T. Giblin, M. Pieroni, and Z. J. Weiner, *Phys. Rev.* **D101**, 083534 (2020), 1909.12842.
- [29] J. Liu, Z.-K. Guo, R.-G. Cai, and G. Shiu, *Phys. Rev. Lett.* **120**, 031301 (2018), 1707.09841.
- [30] J. Liu, Z.-K. Guo, R.-G. Cai, and G. Shiu, *Phys. Rev.* **D99**, 103506 (2019), 1812.09235.
- [31] C. Fu, P. Wu, and H. Yu, *Phys. Rev.* **D97**, 081303 (2018), 1711.10888.
- [32] J. Garcia-Bellido, D. G. Figueroa, and J. Rubio, *Phys. Rev.* **D79**, 063531 (2009), 0812.4624.
- [33] G. Jin, C. Fu, P. Wu, and H. Yu, *Eur. Phys. J.* **C80**, 491 (2020), 2007.02225.
- [34] R. Easther, J. T. Giblin, Jr., and E. A. Lim, *Phys. Rev. Lett.* **99**, 221301 (2007), astro-ph/0612294.
- [35] A. D. Linde, *Phys. Rev.* **D49**, 748 (1994), astro-ph/9307002.
- [36] D. H. Lyth and D. Wands, *Phys. Lett. B* **524**, 5 (2002), hep-ph/0110002.
- [37] A. Bedroya and C. Vafa, *JHEP* **09**, 123 (2020), 1909.11063.
- [38] J. Aasi et al. (LIGO Scientific), *Class. Quant. Grav.* **32**, 074001 (2015), 1411.4547.
- [39] S. Kawamura et al., *Class. Quant. Grav.* **28**, 094011 (2011).
- [40] P. Amaro-Seoane et al. (LISA) (2017), 1702.00786.
- [41] W.-H. Ruan, Z.-K. Guo, R.-G. Cai, and Y.-Z. Zhang (2018), 1807.09495.
- [42] G. N. Felder and I. Tkachev, *Comput. Phys. Commun.* **178**, 929 (2008), hep-ph/0011159.
- [43] A. V. Frolov, *JCAP* **0811**, 009 (2008), 0809.4904.
- [44] D. G. Figueroa, J. Garcia-Bellido, and A. Rajantie, *JCAP* **1111**, 015 (2011), 1110.0337.
- [45] M. A. Amin and D. Shirokoff, *Phys. Rev.* **D81**, 085045 (2010), 1002.3380.
- [46] M. Gleiser and D. Sicilia, *Phys. Rev.* **D80**, 125037 (2009), 0910.5922.
- [47] X.-X. Kou, C. Tian, and S.-Y. Zhou, *Class. Quant. Grav.* **38**, 045005 (2021), 1912.09658.
- [48] K. D. Lozanov and M. A. Amin, *Phys. Rev.* **D97**, 023533 (2018), 1710.06851.
- [49] L. McAllister, E. Silverstein, and A. Westphal, *Phys. Rev.* **D82**, 046003 (2010), 0808.0706.
- [50] E. Silverstein and A. Westphal, *Phys. Rev.* **D78**, 106003 (2008), 0803.3085.